Theor Appl Genet (2011) 122:459–470
DOI 10.1007/s00122-010-1460-0

ORIGINAL PAPER

Characterization and genetic analysis of a low-temperature-sensitive mutant, *sy-2*, in *Capsicum chinense*

Song-Ji An · Devendra Pandeya · Soung-Woo Park · Jinjie Li · Jin-Kyung Kwon · Sota Koeda · Munetaka Hosokawa · Nam-Chon Paek · Doil Choi · Byoung-Cheorl Kang

Received: 16 June 2010 / Accepted: 30 August 2010 / Published online: 1 October 2010
© Springer-Verlag 2010

Abstract A temperature-sensitive mutant of *Capsicum chinense*, *sy-2*, shows a normal developmental phenotype when grown above 24°C. However, when grown at 20°C, *sy-2* exhibits developmental defects, such as chlorophyll deficiency and shrunken leaves. To understand the underlying mechanism of this temperature-dependent response, phenotypic characterization and genetic analysis were performed. The results revealed abnormal chloroplast structures and cell collapse in leaves of the *sy-2* plants grown at 20°C. Moreover, an excessive accumulation of reactive oxygen species (ROS) resulting in cell death was detected in the chlorophyll-deficient sectors of the leaves. However, the expression profile of the ROS scavenging genes did not alter in *sy-2* plants grown at 20°C. A further analysis of fatty acid content in the leaves showed the impaired pathway of linoleic acid (18:2) to linolenic acid (18:3). Additionally, the *Cafad7* gene was downregulated in *sy-2* plants. This change may lead to dramatic physiological disorder and alteration of leaf morphology in *sy-2* plants by losing low-temperature tolerance. Genetic analysis of an F_2 population from a cross between *C. chinense* '*sy-2*' and wild-type *C. chinense* 'No. 3341' showed that the *sy-2* phenotype is controlled by a single recessive gene. Molecular mapping revealed that the *sy-2* gene is located at a genomic region of the pepper linkage group 1, corresponding to the 300 kb region of the Ch1_scaffold 00106 in tomato chromosome 1. Candidate genes in this region will reveal the identity of *sy-2* and the underlying mechanism of the temperature-dependent plant response.

Communicated by M. Havey.

S.-J. An and D. Pandeya contributed equally to this work.

Electronic supplementary material The online version of this article (doi:10.1007/s00122-010-1460-0) contains supplementary material, which is available to authorized users.

S.-J. An · D. Pandeya · S.-W. Park · J. Li · J.-K. Kwon · N.-C. Paek · D. Choi · B.-C. Kang (✉)
Department of Plant Science, Plant Genomics and Breeding Institute, Research Institute for Agriculture and Life Sciences, Seoul National University, 599 Gwanak-ro Gwank-gu, Seoul 151-921, Korea
e-mail: bk54@snu.ac.kr

J. Li
Key Laboratory of Crop Genomics and Genetic Improvement of Ministry of Agriculture, Beijing Key Lab of Crop Genetic Improvement, China Agriculture University, Beijing 100094, China

S. Koeda · M. Hosokawa
Department of Agronomy and Horticultural Science, Graduate School of Agriculture, Kyoto University, Sakyo-ku, Kyoto 606-8502, Japan

Introduction

Pepper (*Capsicum* ssp.), a genus in the Solanaceae family, is one of the most economically important vegetable crops worldwide. Native to the tropics, pepper requires a high temperature during plant development. The optimum growth temperature for pepper is between 25 and 30°C, and temperature change affects various physiological functions and morphological development. When temperature decreases below 15°C, pepper growth is stunted, and bloom and fruit production ceases. Above 32°C, pepper continues to produce flowers, but the fruit set is reduced by a failure of flower abscission, resulting in a significant reduction in pepper production (Erickson and Markhart 2001).

The production of a crop is challenged by abiotic and biotic stresses. Among them, low temperature (LT)

adversely affects the photosynthetic efficiency of a plant, controlling its geographical distribution (Chinnusamy et al. 2007). The severity of both high and low temperature stress is proportional to the cumulative effect of intensity, duration, and rate of temperature change (Sharma et al. 2005; Washid et al. 2007; Thakur et al. 2010). Low temperature can alter multiple aspects of cellular physiology such as membrane fluidity, nucleic acid and protein structure, and metabolite and osmolyte concentrations (Wang et al. 2003; Chinnusamy et al. 2007). Low temperature can also affect plant response to other environmental stresses including drought and osmotic stresses (Rodríguez et al. 2006).

In plants, ROS such as singlet oxygen, superoxide anion radicals, and hydrogen peroxide (H_2O_2) are constantly produced in the chloroplasts, mitochondria, and peroxisomes as the by-products of aerobic reactions in several metabolic processes. When ROS production exceeds the scavenging capacity of these radicals under unfavorable abiotic and biotic stresses, ROS act as cytotoxins inducing necrotic lesions, as well as altering the expression of certain genes in many signaling pathways. This will eventually lead to accelerated cell death resulting in a series of morphological and physiological changes in plants (Apel and Hirt 2004; Ahmad et al. 2008; Li et al. 2010). To prevent photo oxidative damage, phototrophic organisms have evolved to possess several antioxidant enzymes, as well as repair machineries in the chloroplasts and cytoplasm. However, the developmental and genetic regulatory mechanisms for the acquisition of a photoprotective capacity in the chloroplasts, particularly during early leaf development at low-temperature conditions, are largely unknown.

Most plants can withstand low and non-freezing temperatures by a complex adaptive process called cold acclimation. Understanding the mechanisms of how plants sense and respond to specific combinations of stress is a challenging area of research (Suzuki and Mittler 2006). During prolonged exposure to low temperature, many plants are able to alleviate the unfavorable effects of low temperature by cold acclimation which is associated with large scale changes in the transcriptome (Fowler and Thomashow 2002; Chinnusamy et al. 2007; Robinson and Parkin 2008), metabolome (Cook et al. 2004; Gray and Heath 2005), and proteome (Goulas et al. 2006; Herman et al. 2006). Various physiological and biochemical changes, including the alteration of lipid protein in the plasma membrane and carbohydrate compositions, are involved in cold acclimation (Lynch and Steponkus 1986; Gorsuch et al. 2010). Previous studies on cold-regulated (*COR*) genes in several plants suggested that cold acclimation may be related to the expression of cold response genes (Thomashow 1998). The alteration of membrane fluidity was also closely related to low-temperature tolerance (Thomashow 1999). The *fad2* mutant in *Arabidopsis*, deficient in ER 18:1 desaturase, shows a collapse of membrane integrity under low temperature, which leads to an abnormal leaf development and dramatic dwarf phenotype at low-temperature conditions (Kachroo et al. 2001).

The low-temperature response mechanism in plants is still unclear, although many studies have been carried out. In recent years, low-temperature-sensitive mutants have been isolated and characterized in an effort to understand the mechanism of low-temperature response (Kargiotidou et al. 2008). For instance, the *Arabidopsis* mutant *npq1*, which has no xanthophyll cycle, showed the accumulation of extensive photoxidative stress and damage in chloroplasts resulting in the photoinhibition of PSII at low temperature (Harvaux and Kloppstech 2001). The *virescent* mutant in maize has a dysfunction in photosynthesis and displayed a similar phenotype as the *npq1* mutant (Pasini et al. 2005). These results demonstrated that impaired function of the chloroplast by increasing photooxidative damage leads to the inhibition of photosynthesis at low temperature.

Sy-2 is a naturally occurring mutant that was found on Seychelles Island in Africa (Koeda et al. 2009). The *sy-2* plants showed dramatic alteration in leaf morphology when the plants were exposed to low temperature (Koeda et al. 2009). Treatments of various temperature, photoperiod, and light intensity showed that the mutant phenotype was only caused by a low temperature, below 24°C. In addition, abnormal cell expansion and periclinal cell divisions were observed in the *sy-2* mutant (Koeda et al. 2009).

Morphological, anatomical, and biochemical studies, in addition to genetic analyses and molecular mapping of the *sy-2* mutant were performed in order to understand the underlying mechanism of the mutant phenotype and the genetic bases of the *sy-2* mutant.

Materials and methods

Plant materials and growth conditions

The *sy-2* (*C. chinense*), wild type 'No. 3341' (*C. chinense*), and F_2 seeds were provided by Dr. Yazawa (Kyoto University). For the characterization of the *sy-2* mutant plant and genetic mapping, the seeds were sterilized and germinated in an incubator at 30°C. Ten seedlings, 1 week old, were transferred to 26°C chambers with 16 h light and 8 h dark until cotyledons were fully expanded. The seedlings were then transferred to 26 or 20°C chambers. The experiment was repeated for at least three times. For the genetic analysis of *sy-2*, seeds were germinated in 26°C chambers until cotyledons were fully expanded, then 148 plants were transferred to 20°C, and low-temperature hypersensitivity was screened after 14 days.

Quantitative analysis of pigment contents

For chlorophyll and carotenoid extraction, 0.1 g of fresh leaf tissue from the 10-week-old *sy-2* and wild-type plants grown at 20 and 26°C was extracted with 1 ml of ice-cold 80% acetone under dim green light. Plant debris was removed by centrifugation at 12,000*g*. Pigment contents were measured by a spectrophotometer at 470, 645, and 663 nm. The average pigment contents of the samples from three plants were calculated. Total Chl *a*, Chl *b*, and carotenoid contents were calculated using the equation of Lichtenthaler (1987).

Observation of chlorophyll autofluorescence

For the observation of chloroplasts in a mesophyll layer of the plants, the first leaves from three plants each of the 10-week-old *sy-2* and wild-type plants grown at 20 and 26°C were harvested. The apex of the leaves were cut and observed by a confocal laser-scanning microscope (Carl Zeiss-LSM510, Oberkochen, Germany) under 543 nm. Chlorophyll autofluorescence was detected with 685-695 LP.

Light and transmission electron microscopy (TEM)

The second leaves of the 10-week-old *sy-2* and wild-type plants grown at 20 and 26°C were harvested, and the middle portion of each leaf was sectioned. Transmission electron microscopy analysis was carried out as previously described (Li et al. 2010), with some modification. The sliced samples were fixed with a modified Karnovsky's fixative [2% paraformaldehyde and 2% glutaraldehyde in 0.05 M sodium cacodylate buffer (pH 7.2)] and washed three times with 0.05 M sodium cacodylate buffer (pH 7.2) at 4°C for 2 h. The samples were bloc-stained and dehydrated in a gradient alcohol series before transitions and infiltrations were processed. A polymerization reaction was carried out at 70°C for 24 h. The sections were sliced to 60 nm with an ultramicrotome (MT-X, RMC, Tucson, AZ, USA), and stained by 2% uranyl acetate and Reynolds' lead citrate for 7 min each. Samples were then observed in a transmission electron microscope (JEM-1010, JEOL, Japan). Sections (60 μm) were attached to glass slides, stained with 1% (w/v) toluidine blue, and observed in a bright field with a light microscope (Axiophot, Zeiss, Oberkochen, Germany).

Detection of reactive oxygen species (ROS)

Hydrogen peroxide accumulation was detected by 3,3-diaminobenzidine (DAB) staining in detached pepper leaves according to Kariola et al. (2005), with some modifications. The leaves of 5-week-old *sy-2* and wild-type plants grown at 20 and 26°C were cut and vacuum infiltrated with 0.1% 3,3-diaminobenzidine (DAB) solution (Sigma, USA). DAB was solubilized in 10 mM MES buffer (pH 6.5). The samples were incubated at room temperature under continuous light for 8 h. Chlorophyll was completely removed at 80°C in 96% ethanol, and embedded in 50% ethanol for observation. For superoxide detection, the leaves were vacuum-infiltrated with 0.05% nitroblue tetrazolium chloride (NBT) in 0.05 M sodium phosphate buffer (pH 7.5), and then incubated at room temperature under continuous light for 6 h. After incubation, chlorophyll was completely removed at 80°C in 96% ethanol and transferred to fresh 50% ethanol for observation.

RNA extraction and semi-quantitative RT-PCR

Total RNA was extracted from the leaves of *sy-2* plants grown at 20 and 26°C using the TRIzol reagent (Invitrogen, Carlsbad, CA, USA) according to the manufacturer's instructions. Total RNA was then treated with RNAse-free DNase I (Ambion, USA) to remove possible contamination of genomic DNA for RT-PCR. Two micrograms of total RNA was used for each RT reaction. RT products equivalent to 50 ng of total RNA were used in the semi-quantitative RT-PCR. The ROS scavenging genes such as APX6, APXT1 and GST1, and a fatty acid synthetic gene, *Ca fad7*, were amplified with gene-specific primers (Table 1).

Genomic DNA extraction and high-resolution melting (HRM) analysis

Genomic DNA was extracted from young leaves using hexadecyltrimethyl-ammonium bromide (CTAB) method (Kang et al. 2001). For high-resolution melting analysis, genomic DNA was quantified on a Nano-Drop® ND-1000 (Nanodrop Technologies, USA). HRM analysis was performed according to Park et al. (2009). PCR was performed in 20-μl reaction volumes with 50 ng of genomic DNA as a template, 10× HRM buffer (1.5 mM $MgCl_2$, 60 mM KCl, 10 mM Tris–Cl), 2.5 mM dNTPs, 1.25 μM SYTO®9 (Invitrogen, USA), 5 μM of forward and reverse primers, 0.2 units of home-made *Taq* DNA polymerase, and purified as previously reported (Desai and Pfaffle 1995). The PCR was performed with a 4 min hold at 95°C as an initial denaturation step, followed by 50 cycles of 15 s at 95°C, 15 s at 55°C, and 30 s at 72°C. HRM analysis was performed automatically after the PCR and programmed to ramp temperature by 0.1°C/s from 70 to 90°C, after the final extension step. The Rotor Gene 6000, Software version 1.7 (Qiagen, Hilden, Germany) was used to discriminate genotypes.

Table 1 List of the primers used for quantitative RT-PCR and Real time PCR

Genes	Primer sequences (5′–3′)	Product size (bp)	Localization
ROS scavenging genes			
Ascorbate peroxidase			
APX 6	GCAGGAACTTTTGATATTGATGAG	490	Cyt, Chl, Mit
	GTGCCCTATCAGATGGAAGTCCAACC		
APX T1	AACATTCTTCTTCAATGGCTTCTC	444	Chl, Mit
	TTACAAGTCCAGCATTGGCTCCATG		
Glutathione-*S*-transferase			
GST 1	AAGCTGTTAACTTGCTCGAAGGAG	482	Cyt
	GGCATAACTAGAAACACATGTTTC		
Fatty acid synthesis genes			
fad3	GCCAACAACTCATCTGCACC	166	Chl
	ACAATGCTTCGGAATTGCAG		
Cafad7	AAGTTGAACAGCGTTGCTGG	204	ER
	CAGCAAGGGGAAGGGTAGAG		
fad8	CCACCCCCTTTTAAGCTTTC	162	ER
	AAGAGGCCAAACAAGCCAAT		

Cyt cytosol, *Chl* chloroplast, *Mit* mitochondria, *ER* endoplasmic reticulum

Fatty acid analysis

Fatty acid analysis was carried out as described by Komagata and Suzuki (1987), with some modification. Plant tissues were sampled from every three plants of each treatment and ground in liquid nitrogen with a pre-cooled mortar and pestle. One gram of ground sample was then transferred to a Teflon-lined screw-capped tube with 3 ml of NaOH–methanol reagent (15% NaOH in 50% aqueous methanol), and heated at 100°C for 30 min. After heating, the samples were cooled to room temperature, and 4.5 ml of HCl–methanol reagent (25% HCl in methanol) was added. The mixture was heated to 100°C for 15 min, and then cooled to room temperature. The methyl esters of the fatty acids were extracted by adding 4.5 ml of ether–hexane (1:1, vol/vol). The mixtures were gently shaken and allowed to stand for 2 min, before the aqueous (lower) layer was completely removed with a Pasteur pipette. To wash the organic phase, 1 ml of phosphate buffer (pH 11.0) was added and allowed to stand for 3 min. The organic (top) layer was isolated and the fatty acid composition of each compound was determined by gas chromatography.

Genetic mapping of *sy-2*

Genetic mapping of the *sy-2* locus was performed using the 118 individuals of F_2 mapping population derived from wild-type and *sy-2* plants, grown at 20°C. To determine the chromosomal location of the *sy*-2 gene, we used 91 COSII markers, placed on 12 pepper linkage groups (Wu et al. 2006, http://solgenomics.net). After determining the chromosomal location of sy-2, COSII markers located on

Table 2 List of primers linked to the *sy*-2 gene

Marker	Marker type	Primer sequences (5′–3′)	Product size (bp)	Primer status	Recombinants
C2_At1g02560	SNP	GCACTTTTAATTCATGGGATGTACTTGG	98	R	11/108
		GATGATATATACTACCAAAGGAATGCC			
C2_At4g14110	SNP	ATCAGAAAGAACTCGCTGTATGTGC	450	R	16/108
		CATCAAATCTCGCAGTTGGCAC			
C2_At2g15890	SNP	CTGATTCTTTGCTTCTATTTCTGGC	200	R	21/108
		TGTACGCTTGTACGTACCACTACC			
C2_At2g15320	SNP	ACAAGTTGACATGGGGAATAACAGC	380	O	23/108
		AGGTTTCTGTGATTTTAAGCAAAGTTG			
C2_At4g29120	SNP	GAGTTCTTGGGCTTTGGATGG	116	R	3/108
		CGTCTAGGATGGATCGGTACC			
C2_At1g09070	SNP	CTTAGAACTGAAAGGGACACAGG	259	R	5/108
		CACAGATACACAATACTGCGTGAG			

Original COSII markers are indicated by O, and redesigned COSII markers are indicated by R

linkage group 1 (Table 2; Fig. 4) were used for fine mapping. For markers longer than 500 bp, primers were redesigned based on the COSII amplicon sequences used to amplify amplicons less than 250 bp in length. Linkage analysis of molecular markers was performed using the Carthagene 1.0 software (Givry et al. 2005). A minimum LOD score of 3.0 and a maximum distance of 30 cM were used as the threshold values.

Results

Phenotypic characterization of the *sy-2* mutant

The *sy-2* plant exhibited normal leaf phenotype under continuous light at 26°C (Fig. 1a). However, when grown at 20°C, *sy-2* plants showed chlorophyll-deficient, pitted, and shrunken leaves with stunted growth (Fig. 1b, right).

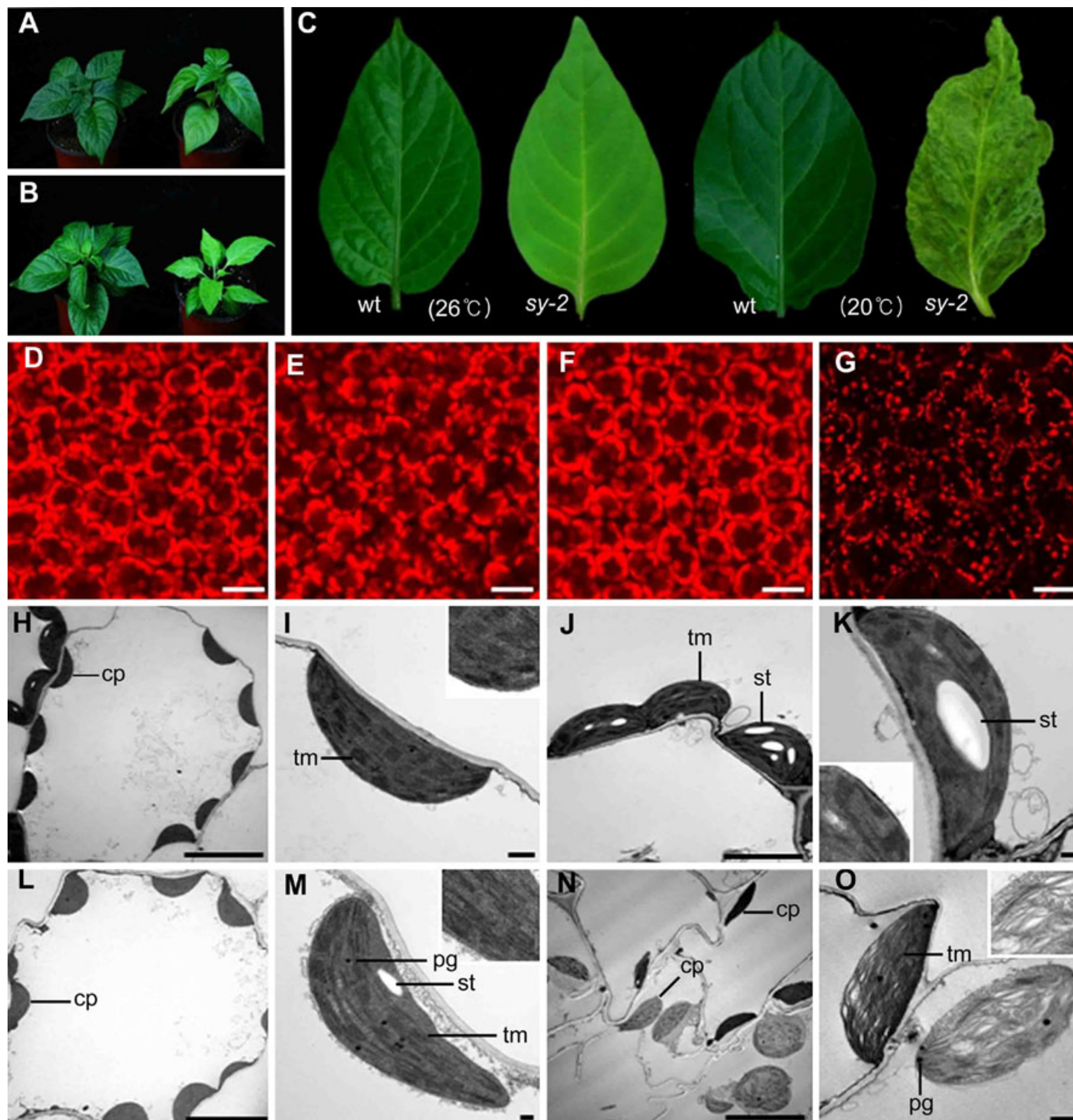

Fig. 1 The phenotypic study and microscopy of *sy-2* plants at different temperature conditions. **a** Wt (*left*) and *sy-2* (*right*) plants grown at 26°C. **b** Wt (*left*) and *sy-2* (*right*) plants grown at 20°C. **c** Leaves of wt and *sy-2* plants under growth conditions of 26 and 20°C. **d–o** Microscopic study of sy-2 leaves at different temperature conditions. **d–g** Confocal microscopic analysis of chloroplasts in mesophyll cells of wt and *sy-2* mutant at 26 and 20°C. **d**, **e** Chlorophyll autofluorescence images of chloroplast in mesophyll cells of the wt and *sy-2* mutant leaves grown at 26°C. **f**, **g** Chlorophyll autofluorescence of chloroplast in mesophyll cells of the wt and sy-2 mutant leaves grown at 20°C. **h–o** Transmission electron microscopic analysis of chloroplasts of wt and the *sy-2* mutant at 26 and 20°C. **h**, **i** and **j**, **k** Chloroplast and thylakoid membranes of mesophyll cells in the leaves of wt and *sy-2* mutant, respectively, at 26°C. **l**, **m** and **n**, **o** Chloroplast and thylakoid membranes of mesophyll cells of wt and the sy-2 mutant, respectively, at 20°C. *Scale bars* represent 1 μm in **d–o**. *cp* chloroplast, *st* starch, *tm* thylakoid membrane, *pg* plastoglobule

Abnormal leaf phenotypes of *sy-2* were observed from first or second emerging leaves after 2 weeks of cold treatment (Fig. 1c, right). Light intensity and temperature conditions were tested to examine whether *sy-2* phenotypes were affected only by temperature. The phenotype of *sy-2* was not affected by light intensity, only by low temperature below 24°C (data not shown). The abnormal leaves of *sy-2* plants developed when the plants were submitted to low temperature did not recover to the normal phenotype after the temperature shift from 20 to 26°C, but new leaf development in sy-2 plants with normal phenotype were observed after temperature shift from 20 to 26°C (data not shown).

Amounts of total chlorophylls and carotenoid contents of wild type and *sy-2* grown at 20 and 26°C were measured (Table 3). The chlorophyll a content was slightly reduced in *sy-2* grown at 20°C compared to wild-type plants. Interestingly, chlorophyll *b* and carotenoid content were significantly reduced in *sy-2* plants at 20°C. However, chlorophyll *a*, chlorophyll *b* and carotenoid contents were not significantly affected in the *sy-2* plants grown at 26°C (Table 3).

Histological observation of *sy-2*

Anatomical study showed that the wild-type plants grown at 26 and 20°C developed a normal leaf phenotype (Online Resource 5). Similarly, the internal structure of those leaves developed normally (Online Resource 5E, G). However, the development of *sy-2* leaves was temperature dependent. At 26°C, *sy*-2 plants developed leaves with normal shape and regular epidermal and mesophyll cells (Online Resource 5B, F), but at 20°C the leaves were deformed showing chlorophyll deficiency and pitted lesions (Online Resource 5D). At 20°C, epidermal cells of *sy-2* leaves were broader, mesophyll cells were irregular and ruptured, and chloroplasts were fewer (Online Resource 5H).

Table 3 Comparison of chlorophyll and carotenoid pigments contents in wild-type and *sy-2* plants

Photosynthetic pigments	Temperature (°C)	Plant	Pigment content (mg/g)
Chl *a*	26	Wt	1.20 ± 0.10
		sy-2	0.97 ± 0.08
	20	Wt	1.08 ± 0.23
		sy-2	0.62 ± 0.14
Chl *b*	26	Wt	0.49 ± 0.11
		sy-2	0.37 ± 0.02
	20	Wt	0.40 ± 0.10
		sy-2	0.20 ± 0.04*
Carotenoid	26	Wt	0.20 ± 0.04
		sy-2	0.20 ± 0.02
	20	Wt	0.21 ± 0.05
		sy-2	0.11 ± 0.03*

The values are the mean ± SD obtained from three independent plants grown at respective temperature conditions

* The significance of difference between wild type and sy-2 at 20°C determined by the Student's *t* test ($P < 0.1$)

Impairment of chloroplast development in *sy-2* mutant

To further investigate whether the deficiency of photosynthetic pigments affect chloroplast development, chloroplasts in mesophyll cells of *sy-2* were analyzed by a confocal fluorescence microscope. There was no significant difference in the chloroplast structure between the leaves of wild-type (Fig. 1d) and *sy-2* plants (Fig. 1f) grown at 26°C. However, a significantly weak signal of red autofluorescence of chlorophyll was observed in the chloroplasts of *sy-2* plants grown at 20°C (Fig. 1g) compared to those of the wild-type plants (Fig. 1e).

The phenotypes of *sy-2* plants indicated that the development of chloroplast structure may be impaired during plant development under 20°C. To test this hypothesis, we performed an electron microscope examination of the leaf tissue of wild-type and *sy-2* plants. The electron microscope observation showed normal chloroplast development in wild type at 26°C (Fig. 1h, i) and 20°C (Fig. 1j, k). Similarly, the chloroplast structure of *sy-2* at 26°C was normal (Fig. 1l, m). However, an abnormally stacked grana structure and indistinct thylakoid membrane layers were observed in the leaf section of *sy-2* plants at 20°C (Fig. 1n–o). These results demonstrate that the development of chloroplasts in *sy-2* plants is affected by low temperature.

Reactive oxygen species (ROS) are highly generated in *sy-2* mutant

To investigate whether the chlorophyll-deficient phenotype of *sy-2* is induced by the increased production of ROS, the accumulation of H_2O_2 and superoxide were examined between the leaves of wild-type and *sy-2* plants using DAB and NBT staining, respectively. In the presence of superoxide a deep blue precipitate is formed when NBT staining is used, and in the presence of H_2O_2 a dark-brown precipitate is formed when DAB staining is used. No significant differences in the production of ROS were observed between the leaves of the wild-type and *sy-2* plants grown at 26°C (Fig. 2a, b, left panel). However, the elevated accumulation of superoxide and H_2O_2 was observed in *sy-2* leaves grown at 20°C (Fig. 2a, b, right panel). The accumulation of superoxide and H_2O_2 was not detected in the leaf tissues of wild-type plants at 26°C (Fig. 2c, g) and

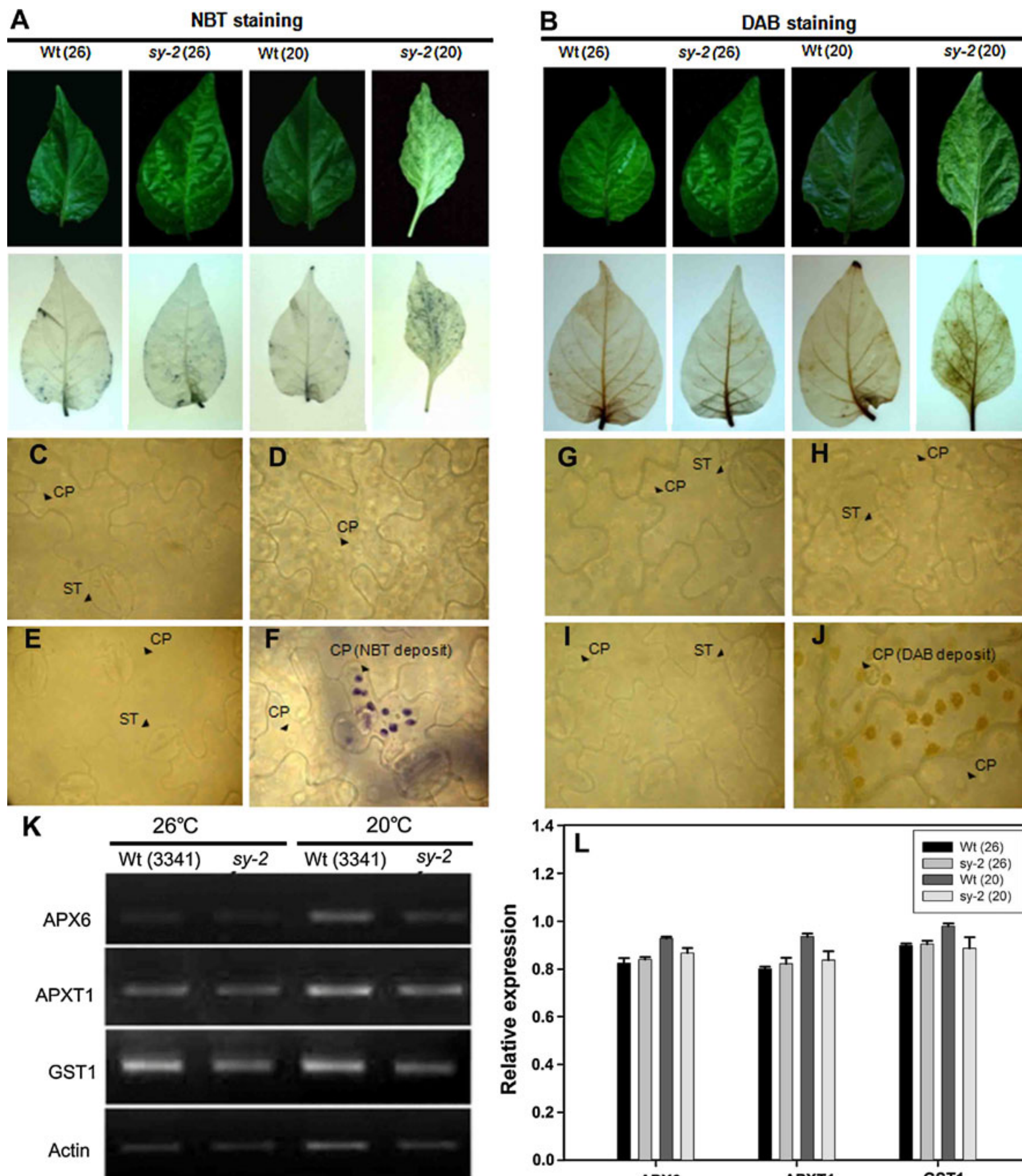

Fig. 2 ROS accumulation and the expression of ROS scavenging genes in *sy-2* leaves. **a** Photographs of leaves before (*first panel*) and after (*second panel*) NBT staining. **b** Photographs of leaves before (*first panel*) and after (*second panel*) DAB staining. The images of leaf section showing chloroplasts in mesophyll cells of NBT-stained wild type at 26°C (**c**) and 20°C (**d**), and *sy-2* at 26°C (**e**) and 20°C (**f**). The images of leaf section showing chloroplasts in mesophyll cells of DAB-stained wild type at 26°C (**g**) and 20°C (**h**), and the *sy-2* at 26°C (**i**) and 20°C (**j**). Dark blue-colored formazan deposits were observed in chloroplasts of the *sy-2* grown at 20°C. The images were taken at 1,000 × magnification. The expression profiles of ROS scavenging genes. K RT-PCR-gel picture showing the expression of different ROS scavenging genes in *sy-2* plants. **l** The expression pattern of ROS scavenging genes (**k**) were quantified. Means and standard deviations were obtained from three independent leaf samples grown at 26 and 20°C

20°C (Fig. 2d, h), and *sy-2* plants at 26°C (Fig. 2e, i), However, microscopic observation of NBT and DAB-stained leaves indicated that at 20°C, the dark blue-colored superoxide deposit (Fig. 2f) and dark brown polymerization deposit of H_2O_2 (Fig. 2j) were located at the chloroplasts of *sy-2*. These results showed that superoxide and H_2O_2 are accumulated in the chloroplast of *sy-2* leaves under low temperature.

The accumulation of ROS in the leaves of *sy-2* mutant plants grown at 20°C suggested that the expression patterns

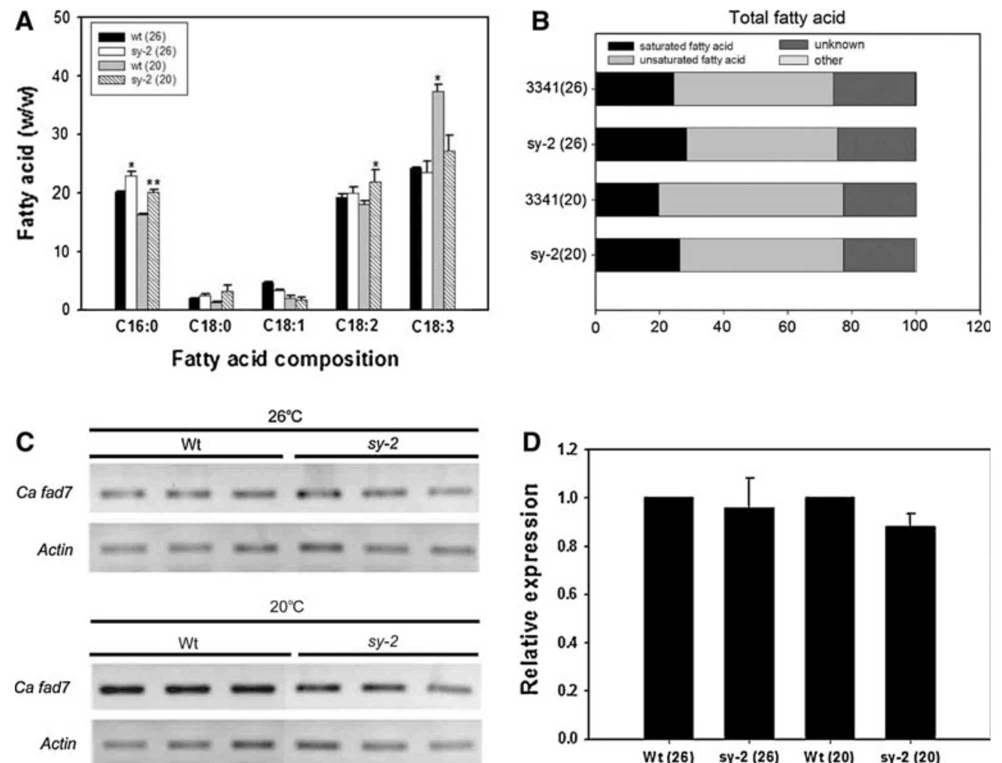

Fig. 3 Study of leaf fatty acid composition and gene expression. **a** Leaf fatty acid composition of wild type and the *sy-2* mutant grown at 26 and 20°C. **b** Total saturated and unsaturated fatty acids, and unknown contents in wild type and the *sy-2* mutant grown at 26 and 20°C. Values are represented as an average % of the total fatty acids obtained from three replicates of wild-type and *sy-2* plants. Expression pattern of the *Cafad7* gene in the *sy-2* mutant. **c** The RT-PCR gel picture and **d** quantified graph of **c** for the expression of *Ca fad7* in wild-type and sy-2 leaves at 26°C (*upper panel*) and 20°C (*lower panel*) obtained from three independent analyses of leaves from individual plants. *Actin* is used as a loading control. *Asterisks* the significance of difference determined by the Student's *t* test (*$P < 0.1$; **$P < 0.01$)

of ROS scavenging genes might be functionally impaired during plant growth and development. To confirm this hypothesis, we performed semi-quantitative RT-PCR with gene-specific primers designed from ROS scavenging genes (Table 1). The results showed that the expression level of APX6 was slightly downregulated at low temperature compared to wild type (Fig. 2k, l). Similarly, the expression levels of thylakoid APXT1 and glutathione-*S*-transferase 1 (*GST1*) were also downregulated in the *sy-2* mutant than in the wild-type plants at 20°C (Fig. 2k, l). These results suggested that the expression of H_2O_2 and O_2^- scavenging genes, APX, and GST were partially affected by low temperature in the *sy-2* mutant.

Cell death was also studied in *sy-2* leaves by trypan blue staining. There were no signals of trypan blue in the leaf sectors of wild-type plants grown at both 26°C (Online Resource 6A, E) and 20°C (Online Resource 6B, F), and the leaf sectors of *sy-2* grown at 26°C (Online Resource 6C, G). However, the dark blue deposits of trypan blue were partially accumulated in *sy-2* leaves grown at 20°C (Online Resource 6D). Under a high magnification, the dark blue deposits of trypan blue were found in the cytoplasm of *sy-2* leaves at 20°C (Online Resource 6H).

Fatty acids are deficient in the sy-2 mutant

Fatty acid composition was measured to test the involvement of fatty acids in the alteration of leaf morphology in *sy-2* plants exposed to low temperature. The results showed that an unsaturated fatty acid, 18:2, content in leaves of *sy-2* plants grown at 20°C was increased compared to the wild-type and *sy-2* plants grown at 26°C (Fig. 3a). The content of another unsaturated fatty acid, 18:3, in *sy-2* leaves was increased slightly at 20°C compared with *sy-2* grown at 26°C. However, the fatty acid content was much less than that of the wild-type plants grown at 20°C. Interestingly, a saturated fatty acid, 16:0, content of *sy-2* plants was significantly increased compared to that of the wild type at 20°C (Fig. 3a; Online Resource 3). The content of the other unsaturated fatty acids (18:0 and 18:1) composition showed no significant difference between wild type and *sy-2* at 26 and 20°C (Fig. 3a). Overall, the content of unsaturated fatty acid in *sy-2* plants decreased significantly compared to that of the wild-type plants at 20°C (Fig. 3b).

To understand whether the biosynthetic pathway of unsaturated fatty acid is impaired under low-temperature conditions, gene expression analysis was performed with the primers designed from unsaturated fatty acid genes, which were selected based on the results of fatty acid composition analysis of *sy-2* (Table 1). The differential expression of *fad7* (linolenic acid, 18:3) between wild type and *sy-2* were observed at 20 and 26°C (Fig. 3c). The expression level of *fad7* was similar in both wild-type and *sy-2* plants at 26°C.(Fig. 3c, d). However, the expression level of *fad7* was reduced in the *sy-2* mutant at 20°C compared with the wild-type plants (Fig. 3c, d). Additionally, we were not able to amplify *fad3* and *fad8* genes

in this experiment (data not shown). These results suggested that the expression of *fad7* was affected by low temperature in the *sy-2* mutant.

Genetic mapping of *sy-2* and candidate gene prediction

Genetic mapping of the *sy-2* locus was performed using the F_2 mapping population derived from wild-type and *sy-2* plants, grown at 20°C. The segregation ratio of the 148 individuals was consistent with the expected ratio of 3 (118 wild type):1 (30 mutant), which is a typical Mendelian segregation ratio of a single recessive gene (Online Resource 2). To determine the chromosomal location of the *sy-2* gene, a total of 91 COSII markers were used. Among them, the COS21 (C2_At2g15890) located on linkage group 1 was found to be linked to the *sy-2* phenotype (21 recombinants out of 108 individuals). To determine the more precise location of *sy*-2 in linkage group 1, six additional markers flanking C2_At2g15890 were tested, and found that *sy-2* is located between C2_At4g29120 and C2_At1g09070 (Fig. 4).

When we compared this region with the tomato genome map EXPEN2000 (Wu et al. 2006) and sequence data base (http://cab.pepper.snu.ac.kr), we found that this region corresponds to the tomato scaffold, Ch01_scaffold00160, spanning about 300 kb, between C2_At4g29120 and C2_At1g09070. In the sequence, 51 genes were predicted by gene prediction FGENESH (http://linux1.softberry.com) and blastx (http://blast.ncbi.nlm.nih.gov). There were several candidate genes including five lipoxygenase genes, heat shock proteins, acyl-CoA6, mevalonate kinase, and other proteins (Online Resource 4).

Discussion

Here we present the phenotypic characterization and genetic analysis of the low-temperature-sensitive mutant, *sy-2* (*C. chinense*). The *sy-2* mutant showed chlorophyll deficiency and abnormal leaf development at low temperatures as described previously by Koeda et al. (2009). The abnormal phenotype was formed at the early stage of leaf development, and the phenotype could not be recovered even after the plants were transferred to a normal temperature condition. However, the *sy-2* phenotype was not observed in the leaves at the fully developed stages. A similar phenotype was observed in the *virescent* mutant in rice, where chlorophyll content was decreased at the early stage of leaf development due to the blocked chloroplast development at a low temperature of 20°C (Iba et al. 1991). These temperature-shift experiments strongly support the notion that the fate of chloroplasts and abnormal leaf phenotype is irreversibly determined during the early stages of leaf development.

The genes related to lipid metabolism, chloroplast function, carbohydrate metabolism, and free radical detoxification play a critical role in plant acclimation to low temperatures (Provart et al. 2003). Photosynthesis is an essential process for the development and survival of photosynthetic organisms (Bryant and Frigaard 2006).

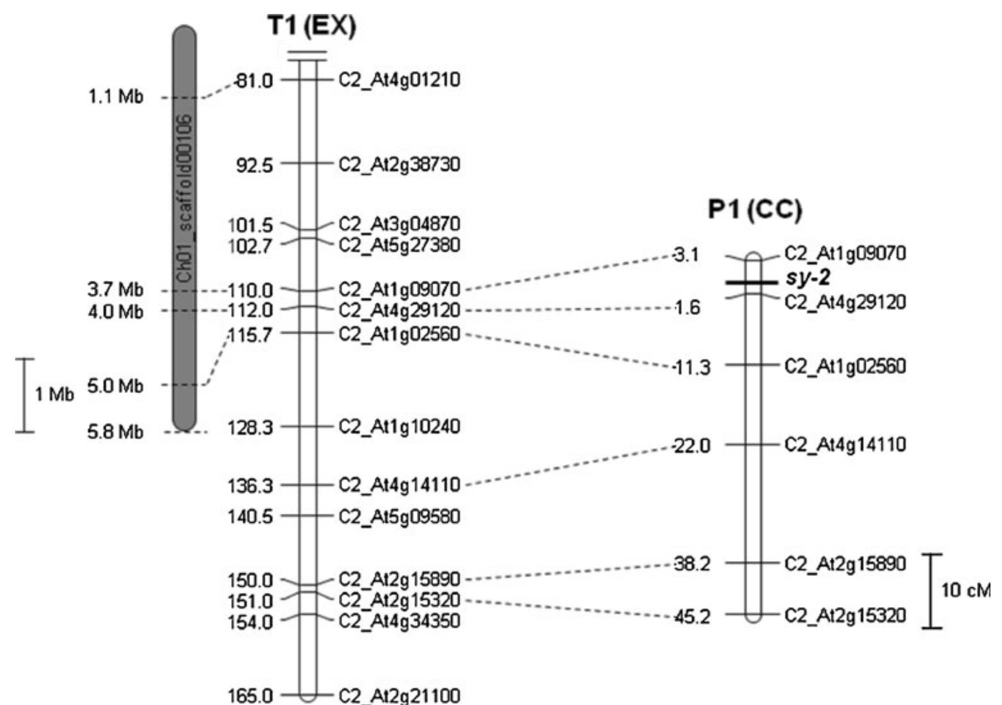

Fig. 4 Genetic mapping of *sy-2*. Two linkage groups corresponding to chromosome 1 of the tomato [*T1* (*EX*)] and pepper [*P1* (*CC*)] genome represent the intraspecific *sy-2* map and tomato EXPEN2000 (Wu et al. 2006). The common COSII markers in the two linkage groups are indicated as *dotted lines*. Tomato scaffold, Ch01_scaffold00106, which is the counterpart of the tomato genetic linkage group, is represented by a *shadow bar* at *left*. The *left scale bar* indicates the physical distance in mega base (*Mb*), and the *right scale bar* indicates the genetic distance in centi Morgan (*cM*)

Carotenoid is one of the photosynthetic pigments, and plays a central role in the protection of chlorophyll against photooxidative damage by environmental stresses (Wilhelm and Helmut 2003). The inhibition of carotenoid biosynthesis leads to a loss of chlorophyll and photoinhibition, and consequently results in chlorophyll-deficient phenotypes (Wu et al. 1997; Aluru et al. 2001). Furthermore, low temperature causes the alteration of chloroplast structure by photooxidative damage or the impairment of photosynthesis by an altered membrane lipid composition of the chloroplast (Pasini et al. 2005; Harvaux and Kloppstech 2001; Wu et al. 1997). An abnormal structure of chloroplasts, as well as fewer and abnormally stacked thylakoid membranes were also observed in a barley *chlorina* mutant at low temperature (Knoetzel and Simpson 1991). In this study, we also observed similar phenotypic changes in the *sy-2* leaves at 20°C, with a reduction of chlorophyll and carotenoid contents, and an abnormal structure of chloroplasts in the chlorophyll-deficient sectors. A reduction of photosynthetic pigments, increased production of superoxide and H_2O_2, and subsequent cell death in chlorophyll-deficient sectors was observed in *sy-2*, similar to the *zn* (*zebra-necrosis*) mutant in rice (Li et al. 2010). In addition, irregular and collapsed cells were also observed in the leaves of *sy-2* plants at 20°C. The mutant phenotype might be due to the oxidative burst caused by the excessive accumulation of ROS.

The accumulation of ROS depends on the expression of ROS scavenging genes (Gechev et al. 2006). The quantitative RT-PCR result revealed that the expression levels of the ROS scavenging genes, *APX6*, *APXT1* and *GST1* were slightly downregulated in *sy-2* mutant leaves than that of the wild-type plants at 20°C. These results strongly suggest that the cell death and leaf deformation in *sy-2* at low temperature is because of the excessive accumulation of ROS which might overwhelm the ROS scavenging activity. Fatty acids contribute to induce stress resistance by adjusting membrane fluidity which depends upon the changing levels of unsaturated fatty acids (Blee 2002). The *Arabidopsis* mosaic death 1 (*mod1*) mutant shows premature cell death and dramatic alterations in plant morphology at 23°C by impaired fatty acid biosynthesis (Mou et al. 2000). A similar phenotype was observed in *Arabidopsis* and cotton *fad2* mutants, deficient in ω-6 desaturase in the endoplasmic reticulum (ER), which has significantly decreased polyunsaturates in the extrachloroplast membrane lipids at low temperature (Miquel et al. 1993). To test whether *sy-2* also shows impaired fatty acid biosynthesis, we analyzed the fatty acid composition of wild type and *sy-2*. Overall, there was a slight difference in the ratio of saturated fatty acid to unsaturated fatty acid at 26°C between wild-type and *sy-2* plants, while there was a big difference at 20°C. During fatty acid biosynthesis, when fatty acid converts from linoleic acid (18:2) to linolenic acid (18:3), the synthesis of linolenic acid (18:3) in *sy-2* was significantly less than that of wild-type plants at 20°C (Fig. 3a; Online Resource 3), indicating that linoleic acid (18:2) to linolenic acid (18:3) pathway might have been impaired in *sy-2*. This result is consistent with previous studies where the reduction of linolenic acid (18:3) was observed in *Arabidopsis* fatty acid synthesis mutants, *fad3*, *7*, and *8* mutants (Iba 2002; Browse et al. 1986; Routaboul et al. 2000). To understand the expression pattern of fatty acid biosynthesis genes, here we compare the mRNA level of *sy-2* to the wild-type plants. The result showed that *Ca fad7* was downregulated in the *sy-2* plants grown at 20°C. This result is consistent with previous reports that when plants are exposed to low temperature, many plants are able to overcome the unfavorable effects of low temperature by changing their gene expression pattern (Fowler and Thomashow 2002; Chinnusamy et al. 2007; Robinson and Parkin 2008; Goulas et al. 2006; Herman et al. 2006) and metabolic activities (Cook et al. 2004; Gray and Heath 2005). Therefore, the failure of the adjustment of the fatty acid composition at low temperature appears to block the expression of the genes which are required for cold acclimatization resulting in various physiological disorders ultimately leading *sy-2* plants to having an increased susceptibility to low temperature.

The genetic contents and organization of the tomato and pepper genome is similar (Wang et al. 2008; Wu et al. 2009). Using the pepper sequence of *sy*-2 linked markers including C2_At4g29120 and C2_At1g09070, we were able to find a tomato scaffold, chr01_scaffold00106 (http://cab.pepper.snu.ac.kr). The part of the tomato scaffold length between C2_At4g29120 and C2_At1g09070 was approximately 300 kb, with a corresponding genetic distance of about 5 cM on the pepper *sy*-2 map (Fig. 4). In this sequence, there were several candidate genes such as lipoxygenase genes, heat shock proteins, acyl-CoA synthase 6, and other proteins (Online Resource 4) that were induced under cold treatment. Among the candidate genes, we propose lipoxygenase (LOXs) as the most probable candidate of *sy-2*. LOXs are crucial for the lipid peroxidation process during plant defense, comprised of the family of non-heme-iron containing fatty acid dioxygenases, which are found in all plants and animals (Brash 1999). Plant LOXs are grouped into 9-LOXs or 13-LOXs, according to the position at which oxygen is incorporated into linoleic acid or linolenic acid, which are the most important substrates for LOX catalysis in plants (Feussner and Wasternack 2002). The results of fatty acid analysis in the *sy-2* mutant revealed that there is a defect in the conversion of linoleic acid to linolenic acid. We predict that the defect in the linoleic acid to linolenic acid pathway might affect the proper function of LOXs, making in *sy-2*

plants become sensitive to low temperature, vulnerable to oxidative damage and cell death. We tried to map sequences of the 4 LOX contigs; however, we were not able to develop a molecular marker for the 4 LOX contigs due to the many copies of the LOX homologous sequence in the pepper genome. Fine mapping of the region will pinpoint the *sy-2* gene. In order to fine map of the *sy-2* region, we are currently developing a larger size of F_2 mapping population.

Acknowledgments This work was carried out with the support of “the BioGreen21 program (Code20070301034022)”, RDA, and by Technology Development Program for Agriculture and Forestry, Ministry for Food, Agriculture, Forestry and Fisheries, Republic of Korea.

References

Ahmad P, Sarwat M, Sharma S (2008) Reactive oxygen species, antioxidants and signaling in plants. J Plant Biol 51:167–173

Aluru MR, Bae H, Wu D, Rodermel SR (2001) The *Arabidopsis immutans* mutation affects plastid differentiation and the morphogenesis of white and green sectors in variegated plants. Plant Physiol 127:67–77

Apel K, Hirt H (2004) Reactive oxygen species: metabolism, oxidative stress, and signal transduction. Annu Rev Plant Biol 55:373–399

Blee E (2002) Impact or phyto-oxylipins in plant defense. Trends Plant Sci 7:315–321

Brash AR (1999) Lipoxygenase: occurrence, functions, catalysis, and acquisition of substrate. J Biol Chem 274:23679–23682

Browse J, Mccourt P, Somerville C (1986) A mutant of Arabidopsis deficient in $C_{18\text{-}3}$ and $C_{16\text{-}3}$ leaf lipids. Plant Physiol 81:859–864

Bryant DA, Frigaard NU (2006) Prokaryotic photosynthesis and phototrophy illuminated. Trends Microbiol 14:488–496

Chinnusamy V, Zhu J, Zhu JK (2007) Cold stress regulation of gene expression in plants. Trends Plant Sci 12:444–451

Cook D, Fowler S, Fiehn O, Thomashow MF (2004) A prominent role for the CBF cold response pathway in configuring the low-temperature metabolome of *Arabidopsis*. PNAS 101: 15243–15248

Desai UJ, Pfaffle PK (1995) Single-step purification of a thermostable DNA polymerase expressed in *Escherichia coli*. Biotechniques 19:780–784

Erickson AN, Markhart AH (2001) Flower production, fruit set, and physiology of bell pepper during elevate temperature and vapor pressure deficit. J Am Soc Hortic Sci 126:697–702

Feussner I, Wasternack C (2002) The lipoxygenase pathway. Annu Rev Plant Biol 53:275–297

Fowler S, Thomashow MF (2002) *Arabidopsis* transcriptome profiling indicates that multiple regulatory pathways are activated during cold acclimation in addition to the CBF cold response pathway. Plant cell 14:1675–1690

Gechev TS, Breusegem FV, Stone JM, Denev I, Laloi C (2006) Reactive oxygen species as signals that modulate plant stress responses and programmed cell death. BioEssay 28:1091–1101

Givry S, Martin B, Patrick C, Denis M, Thomas S (2005) CAR_H^TA GENE: multipopulation integrated genetic and radiation hybrid mapping. Bioinformatics 21:1703–1704

Gorsuch PA, Pandey S, Atkin OK (2010) Temporal heterogeneity of cold acclimation phenotypes in Arabidopsis leaves. Plant Cell Environ 33:244–258

Goulas E, Schubert M, Kieselbach T, Kleczkowski LA, Gardestrom P, Schroder W, Hurry V (2006) The chloroplast lumen and stromal proteomes of *Arabidopsis thaliana* show differential sensitivity to short- and long-term exposure to low temperature. Plant J 47:720–734

Gray GR, Heath D (2005) A global reorganization of the metabolome in *Arabidopsis* during cold acclimation is revealed by metabolic fingerprinting. Physiol Plant 124:236–248

Harvaux M, Kloppstech K (2001) The protective functions of carotenoid and flavonoid pigments against excess visible radiation at chilling temperature investigated in *Arabidopsis npq* and *tt* mutants. Planta 213:953–966

Herman EM, Rotter K, Premakumar R, Elwinger G, Bae R, Ehler-King L, Chen SX, Livingston DP (2006) Additional freeze hardiness in wheat acquired by exposure to −3°C is associated with extensive physiological, morphological, and molecular changes. J Exp Bot 57:3601–3618

Iba K (2002) Acclimative response to temperature stress in higher plants: approaches of gene engineering for temperature tolerance. Annu Rev Plant Biol 53:225–245

Iba K, Takamiya KI, Toh Y, Satoh H, Nishimura M (1991) Formation of functionally active chloroplasts is determined at a limited stage of leaf development in virescent mutants of rice. Dev Genet 12:342–348

Kachroo P, Shanklin J, Shah J, Whittle EJ, Klessig DF (2001) A fatty acid desaturase modulates the activation of defense signaling pathways in plants. PNAS 98:9448–9453

Kang BC, Nahm SH, Huh JH, Yoo HS, Yu JW, Lee MH, Kim BD (2001) An interspecific (*Capsicum annuum* × *C. chinense*) F_2 linkage map in pepper using RFLP and AFLP markers. Theor Appl Genet 102:531–539

Kargiotidou A, Deli D, Galanopoulou D, Tsaftaris A, Farmaki T (2008) Low temperature and light regulate delta 12 fatty acid desaturases (FAD2) at a transcriptional level in cotton (*Gossypium hirsutum*). J Exp Bot 59:2043–2056

Kariola T, Brader G, Li J, Palva ET (2005) Chlorophyllase 1, a damage control enzyme, affects the balance between defense pathways in plants. Plant Cell 17:282–294

Knoetzel J, Simpson D (1991) Expression and organization of antenna proteins in the light-and temperature-sensitive barley mutant *chlorina*. Planta 185:111–123

Koeda S, Hosokawa M, Kang BC, Yazawa S (2009) Dramatic changes in leaf development of the native *Capsicum chinense* from the Seychelles at temperature below 24°C. J Plant Res 122:623–631

Komagata K, Suzuki K (1987) Lipid and cell-wall analysis in bacterial systematic. Methods Microbiol 19:1–67

Li J, Pandeya D, Nath K, Zulfugarov S, Yoo SC, Zhang H, Yoo JH, Cho SW, Koh HJ, Kim DS, Seo HS, Kang BC, Lee CH, Paek NC (2010) Zebra-Necrosis, a thylakoid-bound protein, is critical for photoprotection of developing chloroplasts during early leaf development. Plant J 62:713–725

Lichtenthaler HK (1987) Chlorophyll fluorescence signatures of leaves during the autumnal chlorophyll breakdown. J Plant Physiol 131:101–110

Lynch DV, Steponkus PL (1986) Plasma membrane lipid alterations associated with cold acclimation of winter rye seedlings (*Secale cereale* L. cv Puma). Plant Physiol 83:761–767

Miquel M, James D, Dooner H, Browse J (1993) *Arabidopsis* requires polyunsaturated lipids for low-temperature survival. PNAS 90:6208–6212

Mou Z, He Y, Dai Y, Liu X, Jiayang Li (2000) Deficiency in fatty acid synthase leads to premature cell death and dramatic alterations in plant morphology. Plant Cell 12:405–418

Park SW, An SJ, Yang HB, Kwon JK, Kang BC (2009) Optimization of high resolution melting analysis and discovery of single nucleotide polymorphism in *Capsicum*. Hortic Environ Biotechnol 50:31–39

Pasini L, Bruschini S, Bertoli A, Mazza R, Fracheboud Y, Marocco A (2005) Photosynthetic performance of cold sensitive mutants of maize at low temperature. Physiol Plant 124:362–370

Provart NJ, Gil P, Chen W, Han B, Chang HS, Wang X, Zhu T (2003) Gene expression phenotypes of Arabidopsis associated with sensitivity to low temperatures. Plant Physiol 132:893–906

Robinson SJ, Parkin IAP (2008) Differential SAGE analysis in *Arabidopsis* uncovers increased transcriptome complexity in response to low temperature. BMC Genomics 9:434

Rodríguez M, Canales E, Borroto CJ, Carmona E, López J, Pujol M, Borrás-Hidalgo O (2006) Identification of genes induced upon water-deficit stress in a drought-tolerant rice cultivar. J Plant Physiol 163:577–584

Routaboul JM, Fischer SF, Browse J (2000) Trienoic fatty acids are required to maintain chloroplast function at low temperatures. Plant Physiol 124:1697–1705

Sharma P, Sharma N, Deswal R (2005) The molecular biology of the low-temperature response in plants. BioEssays 27:1048–1059

Suzuki N, Mittler R (2006) Reactive oxygen species and temperature stresses—a delicate balance between signaling and destruction. Physiol Plant 126:45–51

Thakur P, Kumar S, Malik JA, Berger JD, Nayyar H (2010) Cold stress effects on reproductive development in grain crops: an overview. Environ Exp Bot 67:429–443

Thomashow MF (1998) Role of cold-responsive genes in plant freezing tolerance. Plant Physiol 118:1–8

Thomashow MF (1999) Plant cold acclimation: freezing tolerance genes and regulatory mechanisms. Annu Rev Plant Physiol Plant Mol Biol 50:571–599

Wang WX, Vinocur B, Altman A (2003) Plant responses to drought, salinity and extreme temperatures: towards genetic engineering for stress tolerance. Planta 218:1–14

Wang Y, Diehl A, Wu F, Vrebalov J, Giovannoni J, Siepel A, Tanksley SD (2008) Sequencing and comparative analysis of a conserved syntenic segment in the Solanaceae. Genetics 180:391–408

Washid A, Gelani S, Ashraf M, Foolad MR (2007) Heat tolerance in plants: an overview. Environ Exp Bot 61:199–223

Wilhelm S, Helmut S (2003) Antioxidant activity of carotenoids. Mol Aspects Med 24:345–351

Wu J, Lightner J, Warwick N, Browse J (1997) Low-temperature damage and subsequent recovery of *fab1* mutant arabidopsis exposed to 2°C. Plant Physiol 113:347–356

Wu F, Mueller LA, Crouzillat D, Pétiard V, Tanksley SD (2006) Combining bioinformatics and phylogenetics to identify large sets of single-copy orthologous genes (COSII) for comparative, evolutionary and systematic studies: a test case in the euasterid plant clade. Genetics 174:1407–1420

Wu F, Eannetta NT, Xu YM, Durrett R, Mazourek M, Jahn MM, Tanksley SD (2009) A COSII genetic map of the pepper genome provides a detailed picture of synteny with tomato and new insights into recent chromosome evolution in the genus *Capsicum*. Theor Appl Genet 118:927–935